Resonant polaron effect in quantum wells

C. D. Hu and Y.-H. Chang
Department of Physics, National Taiwan University, Taipei, Taiwan 10764, Republic of China
(Received 19 June 1990)

We study the electron-phonon interaction in quantum wells, especially when resonance occurs; that is, when the longitudinal optical-phonon energy is equal to the difference between two subband energies. By using a rather general electron-phonon interaction Hamiltonian and taking into account the confinement of phonons, we calculated the energy shift, level broadening, and effective mass. It was found that the electron-phonon interaction makes a very significant contribution to all of them near resonance.

I. INTRODUCTION

In recent years, there has been much activity[1-19] in the study of electron-phonon interaction in semiconductor heterostructures such as single heterostructure, quantum wells, and superlattices. Interesting phenomena include two-dimensional polarons, cyclotron resonance, and magnetophonon effects. Using the modern molecular-beam-epitaxy technique, one might expect to fabricate high-quality samples and see unambiguous evidence of the electron-phonon interaction. However, there remain still such complications as screening,[3,8,19,12,14] nonparabolicity of subbands,[4,6] temperature dependence[5,8] of effective mass, finite extension of electron wave functions, and confined and interface phonons.[10-18] These effects have been addressed but further effort will be required for better understanding.

The electron-phonon interaction in III-V compounds is in the weak-coupling regime. Therefore most experiments were done under the condition of cyclotron resonance in order that any significant effect might have been seen. Here we propose to study it with subband resonance. That is, an electron occupying a higher subband emits a longitudinal optical (LO) phonon and drops to the first subband. When the energy difference between the subbands is equal to LO-phonon energy, resonance occurs. Hence a large magnetic field is not needed. As we shall show, the electron energy, level broadening, and the effective mass are affected to a large extent by the electron-phonon interaction. Actually, the subband energy and level broadening (transition rate by emitting an LO phonon) had been found to vary with well width in the calculation of Chamberlain and Babiker.[19]

In our study, the forms of the wave functions of electrons and phonons played very important roles. Thus the finite extensions of electrons and confined phonons have to be treated very well. The electron-phonon interaction forms in the literature are not general enough for our purpose. Most theoretical models in the literature can deal with general forms of either electrons or phonons but not both. They[16] also cannot cope with the phonons that have significant dispersions. Here we have derived a very general Hamiltonian for the electron-phonon interaction within the continuum model. It can be used for electrons and phonons of arbitrary wave forms and dispersions (for phonons). It is also very convenient. Therefore we have taken full account of the last two complexities mentioned above. The effect of screening will also be discussed. The derivation will be presented in Sec. II. Calculation details, which involve energy shift, level broadening, and effective mass, are shown in Sec. III and the results will be discussed in Sec. IV.

II. ELECTRON-PHONON INTERACTION

The objective of this section is to establish the form of electron–LO-phonon interaction in the continuum. Though the interaction has been studied for a long time, it is not easy to find expressions for arbitrary electron and phonon forms. Thus the derivation here has its merit. Later in this section, an expression suitable for quantum wells and superlattices will be derived.

An appropriate procedure for phonons is to start with the ion displacements and then work out the second quantization. According to Born and Huang,[20] the interaction Hamiltonian is

$$H_{e\text{-ph}} = -\omega_{\mathrm{LO}} \left[\frac{1}{4\pi} \left[\frac{1}{\epsilon_\infty} - \frac{1}{\epsilon_0} \right] \right]^{1/2} \int d^3r \, \mathbf{d}(\mathbf{r}) \cdot \mathbf{E}_e(\mathbf{r}) \, , \tag{1}$$

where ω_{LO} is the LO-phonon frequency, ϵ_0 and ϵ_∞ are, respectively, the static and high-frequency dielectric constants, $\mathbf{d}(\mathbf{r})$ is the ion displacement multiplied by the square root of the ion mass density, and $\mathbf{E}_e$ is the electric field of free electrons. The second quantization of phonons is standard:

$$\mathbf{d}(\mathbf{r})=\sum_{\mathbf{k}}\left[\frac{\hbar}{2\omega_{\mathbf{k}}}\right]^{1/2}[b_{\mathbf{k}}\mathbf{d}_{\mathbf{k}}(\mathbf{r})+b_{\mathbf{k}}^{\dagger}\mathbf{d}_{\mathbf{k}}^{*}(\mathbf{r})]\ . \tag{2}$$

$\mathbf{d}_{\mathbf{k}}(\mathbf{r})$ and $b_{\mathbf{k}}$ ($b_{\mathbf{k}}^{\dagger}$) are, respectively, the displacement and the annihilation (creation) operator of the phonon mode $\mathbf{k}$. As for electrons, we have

$$\phi(\mathbf{r})=\frac{1}{\Omega}\sum_{\mathbf{q}}\frac{4\pi}{q^2}\rho_{\mathbf{q}}e^{i\mathbf{q}\cdot\mathbf{r}}\ , \tag{3}$$

where Ω is the volume and $\phi(\mathbf{r})$ is the Coulomb potential. $\rho_{\mathbf{q}}$, the charge density, can be quantized as

$$\rho_{\mathbf{q}}=e\sum_{\mathbf{p}}c_{\mathbf{p}-\mathbf{q}}^{\dagger}c_{\mathbf{p}}$$
$$=e\sum_{l,m}c_l^{\dagger}c_m\int d^3\mathbf{r}\,\psi_l^{*}(\mathbf{r})e^{-i\mathbf{q}\cdot\mathbf{r}}\psi_m(\mathbf{r})\ . \tag{4}$$

c_m ($c_m^{\dagger}$) is the annihilation (creation) of the electron at state m and $\psi_m(\mathbf{r})$ is the wave function. With use of integration by parts and Eqs. (2)–(4), Eq. (1) can be rewritten as

$$H_{e\text{-ph}}=\frac{e\omega_{\mathrm{LO}}}{\Omega}\left[\frac{1}{4\pi}\left[\frac{1}{\epsilon_\infty}-\frac{1}{\epsilon_0}\right]\right]^{1/2}\sum_{l,m,\mathbf{k},\mathbf{q}}\left[\frac{\hbar}{2\omega_{\mathbf{k}}}\right]^{1/2}\frac{4\pi}{q^2}\left[\int d^3\mathbf{r}'\,\psi_l^{*}(\mathbf{r}')e^{-i\mathbf{q}\cdot\mathbf{r}'}\psi_m(\mathbf{r}')\right]c_l^{\dagger}c_m$$
$$\times\left[b_{\mathbf{k}}\int d^3\mathbf{r}\,e^{i\mathbf{q}\cdot\mathbf{r}}\nabla\cdot\mathbf{d}_{\mathbf{k}}(\mathbf{r})+b_{\mathbf{k}}^{\dagger}\int d^3r\,e^{i\mathbf{q}\cdot\mathbf{r}}\nabla\cdot\mathbf{d}_{\mathbf{k}}^{*}(\mathbf{r})\right]\ . \tag{5}$$

Thus we have derived the electron-phonon interaction for the arbitrary wave form of electrons and phonons. If both the electron and phonon have a plane wave as their wave function, then Eq. (5) is reduced to

$$H_{e\text{-ph}}=-ie\omega_{\mathrm{LO}}\left[\frac{1}{\epsilon_\infty}-\frac{1}{\epsilon_0}\right]^{1/2}\sum_{\mathbf{q}}\left[\frac{2\pi\hbar}{\Omega\omega_{\mathbf{q}}}\right]^{1/2}\frac{1}{q}(c_{\mathbf{p}-\mathbf{q}}^{\dagger}c_{\mathbf{p}}b_{-\mathbf{q}}+c_{\mathbf{p}-\mathbf{q}}^{\dagger}c_{\mathbf{p}}b_{\mathbf{q}}^{\dagger})\ . \tag{6}$$

For quantum wells and superlattices, one can take advantage of the translational invariance parallel to the interfaces. The wave functions of electrons and phonons are plane waves multiplied by functions of $\mathbf{z}$, which is the coordinate normal to the interfaces:

$$\psi_m(\mathbf{r})=Z_i(z)e^{i\mathbf{p}_{\parallel}\cdot\rho}/\sqrt{A}\ , \tag{7}$$

$$\mathbf{d}_{\mathbf{k}}(\mathbf{r})=\mathbf{U}_n(z,\mathbf{k}_{\parallel})e^{i\mathbf{k}_{\parallel}\cdot\rho}/\sqrt{A}\ , \tag{8}$$

where A is the area of the system and $\mathbf{p}_{\parallel}$ and $\mathbf{k}_{\parallel}$ are wave vectors parallel to the interfaces. Using Eqs. (7) and (8), Eq. (5) becomes

$$H_{e\text{-ph}}=e\omega_{\mathrm{LO}}\left[\frac{1}{\epsilon_\infty}-\frac{1}{\epsilon_0}\right]^{1/2}\sum_{i,j,n,\mathbf{q}}\left[\frac{2\pi\hbar}{A\omega_{\mathbf{q}_{\parallel},n}}\right]^{1/2}\frac{1}{q^2}\left[\frac{1}{L}\int dz'\,Z_j(z')e^{-iq_zz'}Z_i(z')\right]$$
$$\times c_{i,\mathbf{p}_{\parallel}-\mathbf{q}_{\parallel}}^{\dagger}c_{i,\mathbf{p}_{\parallel}}\left[b_{-\mathbf{q}_{\parallel},n}\int dz\,e^{iq_zz}\left[i\mathbf{q}_{\parallel}\cdot\mathbf{U}_n(z,\mathbf{q}_{\parallel})+\frac{\partial}{\partial z}U_{nz}(z,\mathbf{q}_{\parallel})\right]\right.$$
$$\left.+b_{\mathbf{q}_{\parallel},n}^{\dagger}\int dz\,e^{iq_zz}\left[-i\mathbf{q}_{\parallel}\cdot\mathbf{U}_n^{*}(z,\mathbf{q}_{\parallel})+\frac{\partial}{\partial z}U_{nz}^{*}(z,\mathbf{q}_{\parallel})\right]\right]\ , \tag{9}$$

where L is the width of the system. In the following section, we shall give some details of how $\omega_{\mathbf{q}_{\parallel},n}$, $Z_i(z)$ and $\mathbf{U}_n(z,\mathbf{k}_{\parallel})$ are calculated. Let us conclude this section by noting that, although Eqs. (5) and (9) were derived using the continuum model, they can be applied to other models with a little modification.

III. CALCULATION

In this section we present the forms of the electron wave functions and phonon displacements and how the electron self-energy is calculated close to resonance. While our system is a double heterostructure (DHS) of AlAs/GaAs/AlAs, the method can be applied to any DHS of other different materials.

For electrons, the potential is

$$V(z)=\begin{cases}0, & -L/2<z<L/2\\ V_B, & |z|>L/2\end{cases} \tag{10}$$

where V_B is about 60% of the band gap between GaAs and AlAs. The wave function $Z_i(z)$ is calculated by requiring the $Z_i(z)$ and the flux[21] be continuous at $|z|=L/2$. As a result,

$$Z_i(z)=\begin{cases}c_s\cos(p_iz), & |z|<L/2\\ c_s\cos(p_iL/2)e^{-p_i'(|z|-L/2)}, & |z|>L/2\ ;\end{cases} \tag{11}$$

$$Z_i(z)=\begin{cases} c_a \sin(p_i z), & |z|<L/2 \\ c_a \mathrm{sgn}(z)\sin(p_i L/2)e^{-p_i'(|z|-L/2)}, & |z|>L/2 \end{cases} . \quad (12)$$

Equations (11) and (12) show the symmetric and antisymmetric wave functions, respectively, and c_s and c_a are their normalization constants. p_i and p_i' are related by the following equations:

$$\frac{p_i'}{m_2^*}=\frac{p_i}{m_1^*}\tan(p_i L/2) \quad (13)$$

for symmetric solutions and

$$\frac{p_i'}{m_2^*}=-\frac{p_i}{m_i^*}\cot(p_i L/2) \quad (14)$$

for antisymmetric solutions. m_1^* and m_2^* are the electron effective masses in GaAs and AlAs, respectively. The energy ε_i is given by

$$\varepsilon_i=\frac{\hbar^2 p_i^2}{2m_1^*}=V_B-\frac{\hbar^2 p_i'^2}{2m_2^*} . \quad (15)$$

The bulk GaAs LO-phonon dispersion can be approximated by

$$\omega_{\mathbf{k}}^2=\omega_{\mathrm{LO}}^2-v^2k^2 , \quad (16)$$

where v is the phonon propagating speed. In DHS, the phonons above split into many branches. Each penetrates into the AlAs and becomes an evanescent wave. It is similar to the situation in superlattices where zone folding occurs. However, the ω_{LO} in GaAs is around 296 cm^{-1}. It is much smaller than that in AlAs, which is 360 cm^{-1}. Therefore, the phonon evanescent waves in AlAs decay rather rapidly. We can safely approximate LO phonons in GaAs by completely confined waves. The form of the nth branch phonon is given by

$$\mathbf{U}_n(z,\mathbf{k}_\parallel)=\begin{cases} \dfrac{1}{\sqrt{2L}}\left[\dfrac{\mathbf{k}_\parallel+\mathbf{k}_n}{k}e^{ik_n z}+\dfrac{\mathbf{k}_\parallel-\mathbf{k}_n}{k}e^{-ik_n z}\right] \\ \qquad \text{for symmetric phonons} , \\ \dfrac{1}{\sqrt{2L}}\left[\dfrac{\mathbf{k}_\parallel+\mathbf{k}_n}{k}e^{ik_n z}-\dfrac{\mathbf{k}_\parallel-\mathbf{k}_n}{k}e^{-ik_n z}\right] \\ \qquad \text{for antisymmetric phonons} , \end{cases} \quad (17)$$

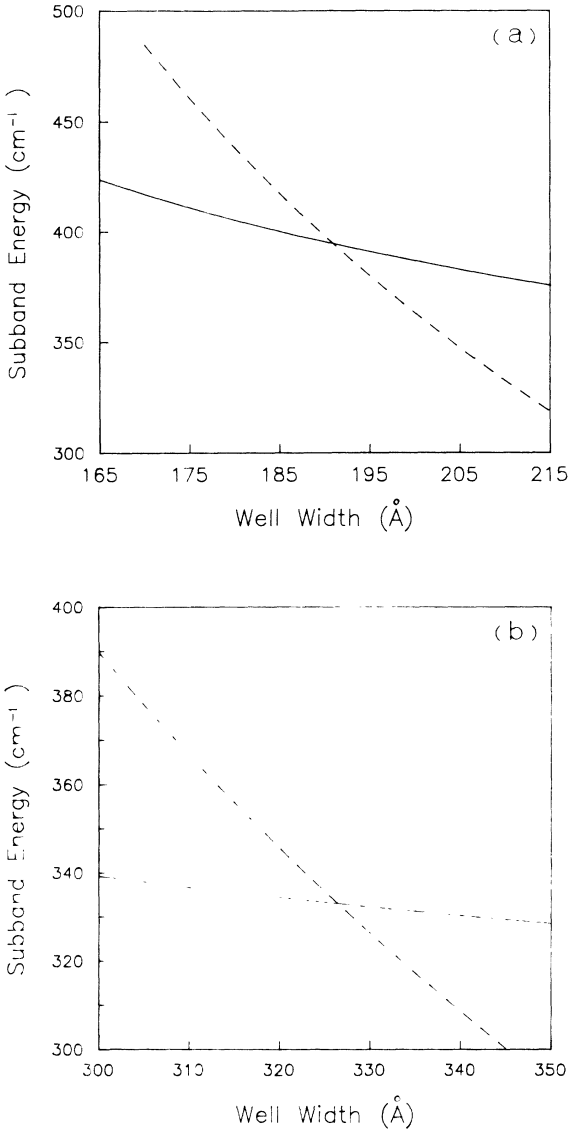

FIG. 1. (a) The first subband energy plus $\hbar\omega_{\mathrm{LO}}$ (solid line) and the second subband energy (dashed line) are plotted against the well width. (b) The first subband energy plus $\hbar\omega_{\mathrm{LO}}$ (solid line) and the third subband energy (dashed line) are plotted against the well width.

where

$$\mathbf{k}=\mathbf{k}_\parallel+\mathbf{k}_n , \quad (18)$$

and $\mathbf{k}_n$, pointing to the z direction, is

$$k_n=n\pi/L . \quad (19)$$

Here, n is odd for symmetric phonons and even for antisymmetric phonons. These phonon forms are almost the same as those derived by Babiker's model.[22]

The electron self-energy of the ith state due to the electron–LO-phonon interaction is given by

$$\Sigma(E,i,\mathbf{p}_\parallel)=\frac{e^2\omega_{\rm LO}^2}{A}\left[\frac{1}{\epsilon_\infty}-\frac{1}{\epsilon_0}\right]\sum_{\mathbf{q},j,n}\frac{2\pi\hbar}{\omega_{\mathbf{q}_\parallel,n}}\frac{1}{q^4}\left|\frac{1}{L}\int dz'\,Z_j^*(z')e^{-iq_z z'}Z_i(z')\right|^2$$
$$\times\left[\left|\int dz\,e^{iq_z z}\left[i\mathbf{q}_\parallel\cdot\mathbf{U}_n^*(z,\mathbf{q}_\parallel)+\frac{\partial}{\partial z}U_{n,z}(z,\mathbf{q}_\parallel)\right]\right|^2\right.$$
$$\times\frac{f_{j,\mathbf{p}_\parallel-\mathbf{q}_\parallel}}{E-\varepsilon_j-\hbar^2(\mathbf{q}_\parallel^2-2\mathbf{p}_\parallel\cdot\mathbf{q}_\parallel)/2m_1^*+\hbar\omega_{\mathbf{q}_\parallel,n}-i\eta}$$
$$+\left|\int dz\,e^{iq_z z}\left[-i\mathbf{q}_\parallel\cdot\mathbf{U}_n^*(z,\mathbf{q}_\parallel)+\frac{\partial}{\partial z}U_{n,z}^*(z,\mathbf{q}_\parallel)\right]\right|^2$$
$$\left.\times\frac{(1-f_{j,\mathbf{p}_\parallel-\mathbf{q}_\parallel})}{E-\varepsilon_j-\hbar^2(\mathbf{q}_\parallel^2-2\mathbf{p}_\parallel\cdot\mathbf{q}_\parallel)/2m_1^*-\hbar\omega_{\mathbf{q}_\parallel,n}+i\eta}\right] \tag{20}$$

according to Eq. (9). Here, $f_{j,\mathbf{p}_\parallel-\mathbf{q}_\parallel}$ is the Fermi function. What concerns us are electrons, not holes; thus $f_{j,\mathbf{p}_\parallel-\mathbf{q}_\parallel}=0$ at 0 K. The resonance at the band edge occurs when $\varepsilon_i-\varepsilon_j\approx\hbar\omega_{\mathbf{q}}$. Since LO phonons are almost dispersionless, one can only achieve resonance by varying electron-energy levels. This can be done by varying well width. Figures 1(a) and 1(b) shows the energy of the first subband plus $\hbar\omega_{\mathbf{q}}$ and the second and third subband energies, respectively, as functions of well width. Clearly, resonances occur around $L=189$ Å for the second subband and $L=323$ Å for the third subband. Keeping only the resonance term, Eq. (20) becomes

$$\Sigma(E,i,\mathbf{p}_\parallel)=\frac{2e^2\omega_{\rm LO}^2}{\Omega}\left[\frac{1}{\epsilon_\infty}-\frac{1}{\epsilon_0}\right]\sum_{\mathbf{q}_\parallel,n}\frac{2\pi\hbar}{\omega_{\mathbf{q}_\parallel,n}}\frac{M_n^2}{q_\parallel^2+k_n^2}\frac{1}{E-\epsilon_1-\hbar^2(\mathbf{q}_\parallel^2-2\mathbf{p}_\parallel\cdot\mathbf{q}_\parallel)/2m_1^*-\hbar\omega_{\mathbf{q}_\parallel,n}+i\eta}\,, \tag{21}$$

where Eqs. (11) and (17) were used. The following approximations were also made:

$$\frac{2\sin(kL/2)}{k}\approx L\delta_k,\quad \omega_{\mathbf{q}_\parallel,n}\approx\omega_{0,n}\equiv\omega_n\,.$$

They are very good approximations when k_n or $q_\parallel$ is small. When k_n or $q_\parallel$ is large the coupling is weak, as Eq. (21) shows. Therefore the above approximations would not introduce any significant error.[23] Finally,

$$M_n=\frac{1}{2}\left[\frac{\sin(p_1+k_n-p_3)L/2}{p_1+k_n-p_3}+\frac{\sin(p_1-k_n+p_3)L/2}{p_1-k_n+p_3}+\frac{\sin(p_1+k_n+p_3)L/2}{p_1+k_n+p_3}+\frac{\sin(p_1-k_n-p_3)L/2}{p_1-k_n-p_3}\right.$$
$$\left.+4\cos(p_1L/2)\cos(p_3L/2)\frac{(p_1'+p_3')\cos(k_nL/2)-k_n\sin(k_nL/2)}{(p_1'+p_3')^2+k_n^2}\right]$$
$$\times\left[\frac{L}{2}+\frac{\sin(p_1L)}{2p_1}+\frac{\cos^2(p_1L/2)}{p_1'}\right]^{-1/2}\left[\frac{L}{2}+\frac{\sin(p_3L)}{2p_3}+\frac{\cos^2(p_3L/2)}{p_3'}\right]^{-1/2}, \tag{22a}$$

for symmetric phonons,

$$M_n=\frac{1}{2}\left[\frac{\sin(p_1+k_n-p_3)L/2}{p_1+k_n-p_3}+\frac{\sin(p_1-k_n+p_3)L/2}{p_1-k_n+p_3}-\frac{\sin(p_1+k_n+p_3)L/2}{p_1+k_n+p_3}-\frac{\sin(p_1-k_n-p_3)L/2}{p_1-k_n-p_3}\right.$$
$$\left.+4\cos(p_1L/2)\cos(p_3L/2)\frac{(p_1'+p_3')\sin(k_nL/2)+k_n\cos(k_nL/2)}{(p_1'+p_3')^2+k_n^2}\right]$$
$$\times\left[\frac{L}{2}-\frac{\sin(p_1L)}{2p_1}+\frac{\sin^2(p_1L/2)}{p_1'}\right]^{-1/2}\left[\frac{L}{2}-\frac{\sin(p_3L)}{2p_3}+\frac{\sin^2(p_3L/2)}{p_3'}\right]^{-1/2}, \tag{22b}$$

for antisymmetric phonons. A glance at Eq. (9) tells us that the transition between the first and second subbands involves antisymmetric phonons and the transition between the first and third subbands involves symmetric phonons. The real part of the self-energy gives the energy shift of the second and third subbands. The imaginary part gives the level broadening. Its derivative with respect to $p_\parallel^2$ at $p_\parallel=0$ gives the effective-mass modification. Their forms are

$$\mathrm{Re}\Sigma(E,i,0)=\frac{e^2\hbar\omega_{\mathrm{LO}}^2}{L}\left[\frac{1}{\epsilon_\infty}-\frac{1}{\epsilon_0}\right]\sum_n\frac{1}{\omega_n}\frac{M_n^2}{E-\epsilon_1-\hbar\omega_n+\hbar^2k_n^2/2m_1^*}\ln\left|\frac{q_B^2(E-\epsilon_1-\hbar\omega_n)}{k_n^2[\hbar^2(q_B^2-k_n^2)/2m_1^*-(E-\epsilon_1-\hbar\omega_n)]}\right|, \tag{23}$$

$$\mathrm{Im}\Sigma(E,i,0)=\frac{-\pi e^2\hbar\omega_{\mathrm{LO}}^2}{L}\left[\frac{1}{\epsilon_\infty}-\frac{1}{\epsilon_0}\right]\sum_n{}'\frac{1}{\omega_n}\frac{M_n^2}{E-\epsilon_1-\hbar\omega_n+\hbar^2k_n^2/2m_1^*}, \tag{24}$$

$$\begin{aligned}\frac{m_1^*}{m^*}-1&=\frac{2m_1^*}{\hbar^2}\left.\frac{\partial\Sigma(E,i,p_\parallel)}{\partial p_\parallel^2}\right|_{p_\parallel=0}\\&=\frac{2m_1^*}{\hbar^2}\frac{e^2\hbar\omega_{\mathrm{LO}}^2}{L}\left[\frac{1}{\epsilon_\infty}-\frac{1}{\epsilon_0}\right]\sum_n\frac{M_n^2}{\omega_n}\left[\frac{\Delta q^2-k_n^2-(k_n^2+\Delta q^2)m_1^*/m^*}{(k_n^2+\Delta q^2)^3}\ln\left|\frac{q_B^2\Delta q^2}{k_n^2\Delta q_B^2}\right|\right.\\&\quad+\frac{1}{q_B^4\Delta q^2(k_n^2+\Delta q^2)}\left[\frac{k_n^4(\Delta q_B^2)^2}{(k_n^2+\Delta q^2)^2}+2k_n^2(q_B^2-k_n^2)\right.\\&\quad\left.\left.+\frac{(q_B^2-k_n^2)^2(q_n^2+\Delta q^2)^2}{(\Delta q_B^2)^2}\right]\right.\\&\quad-\left[1-\frac{m_1^*}{m^*}\right]\frac{1}{q_B^2\Delta q^2(k_n^2+\Delta q^2)}\left[\frac{k_n^2\Delta q_B^2}{k_n^2+\Delta q^2}+\frac{(q_B^2-k_n^2)(k_n^2+\Delta q^2)}{\Delta q_B^2}\right]\\&\quad\left.-\frac{1}{(k_n^2+\Delta q^2)^2}\left[\frac{\Delta q^2}{k_n^2+\Delta q^2}+1-\frac{m_1^*}{m^*}\right]\right],\quad\text{if }\Delta q^2<0\ ;\end{aligned} \tag{25a}$$

$$\begin{aligned}\frac{m_1^*}{m^*}-1&=\frac{2m_1^*}{\hbar^2}\frac{e^2\hbar\omega_{\mathrm{LO}}^2}{L}\left[\frac{1}{\epsilon_\infty}-\frac{1}{\epsilon_0}\right]\sum_n\frac{M_n^2}{\omega_n}\left\{\frac{\Delta q^2-k_n^2-(k_n^2+\Delta q^2)m_1^*/m^*}{(k_n^2+\Delta q^2)^3}\ln\left|\frac{q_B^2\Delta q^2}{k_n^2\Delta q_B^2}\right|\right.\\&\quad+\frac{1}{q_B^4\Delta q^2(k_n^2+\Delta q^2)}\left[\frac{k_n^4(\Delta q_B^2)^2}{(k_n^2+\Delta q^2)^2}+2k_n^2(q_B^2-k_n^2)\right.\\&\quad\left.+\frac{(q_B^2-k_n^2)^2(q_n^2+\Delta q^2)^2}{(\Delta q_B^2)^2}\right]\\&\quad-\left[1-\frac{m_1^*}{m^*}\right]\frac{1}{q_B^2\Delta q^2(k_n^2+\Delta q^2)}\left[\frac{k_n^2\Delta q_B^2}{k_n^2+\Delta q^2}+\frac{(q_B^2-k_n^2)(k_n^2+\Delta q^2)}{\Delta q_B^2}\right]\\&\quad+\frac{1}{(k_n^2+\Delta q^2)^2}\left[\frac{k_n^2}{k_n^2+\Delta q^2}+\frac{k_n^2}{\Delta q^2}-\left[1-\frac{m_1^*}{m^*}\right]\left[2+\frac{k_n^2}{\Delta q^2}\right]\right]\\&\quad\left.-\left[1+\frac{m_1^*}{m^*}\right]\frac{1}{\Delta q^2(k_n^2+\Delta q^2)}\right\},\quad\text{if }\Delta q^2>0\ ;\end{aligned} \tag{25b}$$

where

$$q_B\equiv\frac{\pi}{a}, \tag{26}$$

$$\Delta q^2\equiv 2m_1^*(E-\epsilon_1-\hbar\omega_n)/\hbar^2, \tag{27}$$

$$\Delta q_B^2\equiv q_B^2-k_n^2-\Delta q^2, \tag{28}$$

and a is the lattice constant of GaAs. The summation in Eq. (24) is for $E-\epsilon_1>\hbar\omega_n>E-\epsilon_1-\hbar^2q_B^2/2m_1^*$. Equation (23) was solved first for E. Then it was substituted into Eqs. (24) and (25) to calculate $\mathrm{Im}\Sigma(E,i,0)$ and solve for m^*, respectively.

IV. RESULTS AND DISCUSSION

The parameters we used for calculation are listed in Table I. The phonon speed v is chosen so that the phonon frequency is equal to 250 cm^{-1} when $k=\pi/a$, where a is the lattice constant of GaAs. The strength of electron-phonon coupling is represented by

$$\alpha=\frac{e^2}{\hbar}\left[\frac{1}{\epsilon_\infty}-\frac{1}{\epsilon_0}\right]\left[\frac{m_1^*}{2\hbar\omega_{\mathrm{LO}}}\right]^{1/2}. \tag{29}$$

It was set to be[24] 0.05. The results are shown in Figs. 2 and 3 for the second and third subbands, respectively. In

TABLE I. m_1^* and m_2^* are the effective masses of electrons in GaAs and AlAs, respectively. m_e is the free-electron mass. V_B is the potential barrier of AlAs relative to GaAs. ω_{LO} and v are, respectively, the frequency and speed of LO phonons in GaAs. α was defined in Eq. (29). a is the lattice constant of GaAs.

m_1^*	m_2^*	V_B	ω_{LO}	v	α	a
$0.067m_e$	$0.15m_e$	0.915 eV	296 cm^{-1}	5.376×10^5 cm/s	0.05	5.6533 Å

the upper panel, the real and imaginary parts of the self-energy are shown by the solid and dashed lines, respectively. The lower panel shows the effective mass. It is very clear where resonance occurs. The energy-level shift of $Re\Sigma$ can be more than 6 cm^{-1}. It is more than 4 cm^{-1} in a wide range. This is certainly detectable with experiments such as photoluminescence excitation.

The variation of $Im\Sigma(E)$ can be explained as the following. The first subband state can have a finite momentum $\mathbf{q}_\parallel$ parallel to the interfaces. In a narrow well the energy difference between the first and the upper (the second or third) subbands is greater than $\hbar\omega_{LO}$. An energy-conserved transition can always occur for some $|\mathbf{q}_\parallel|$. Thus $Im\Sigma(E)$ is finite. As the well becomes wider, $Im\Sigma(E)$ drops to zero when E becomes less than $\epsilon_1+\hbar\omega_{LO}$. Now the transition cannot occur without violating energy conservation. Figures 2 and 3 show that this resonance gives a level broadening of the order of 4 cm^{-1}. This can easily be distinguished from the off-resonance case, especially since the electron–LO-phonon interaction is the dominant mechanism for the higher subband electrons to descend to the first subband. It is also interesting to note that the second and third subbands have much sharper levels when the well width is greater than 189 and 323 Å, respectively.

The variation of effective mass is also very interesting. Usually, the effective-mass modification is $\pi\alpha/8$ for two-dimensional systems and $\alpha/6$ for three-dimensional systems;[25] that is, around 1%. Here m^* diverges near resonance. It is more comprehensible to study the inverse of the effective mass, i.e., $\partial E/\partial p_\parallel^2$. We propose the following picture. The higher subband with parallel momentum $\mathbf{p}_\parallel$ forms a parabolic band. The first subband and a LO phonon form another band. Also remember that the electron-phonon interaction shifts the energy level downward. As we approached resonance from the small-well-width side, the parabolic band descended from above to the band with phonons. The bottom of the parabolic band was pulled down more because it was closer to resonance. Thus $1/m^*$ became greater. If we had started with the large well width, then the parabolic band would have moved upward toward resonance. The

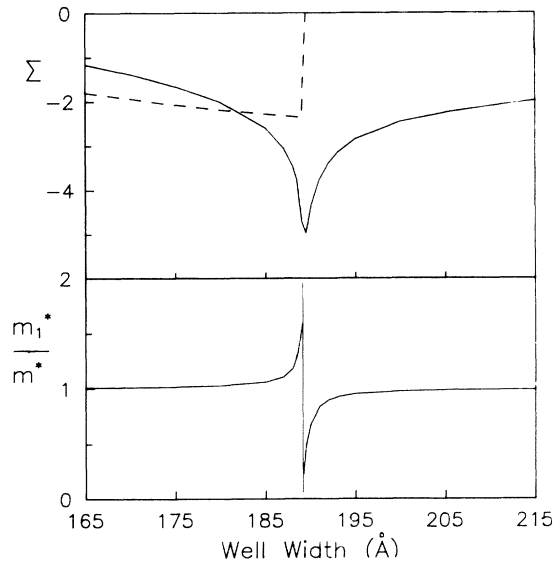

FIG. 2. Upper panel: the real part (solid line) and imaginary part (dashed line) of the self-energy of the second subband are plotted as functions of well width. Lower panel: the ratio between the effective masses of the second subband with and without electron-phonon coupling is plotted against the well width.

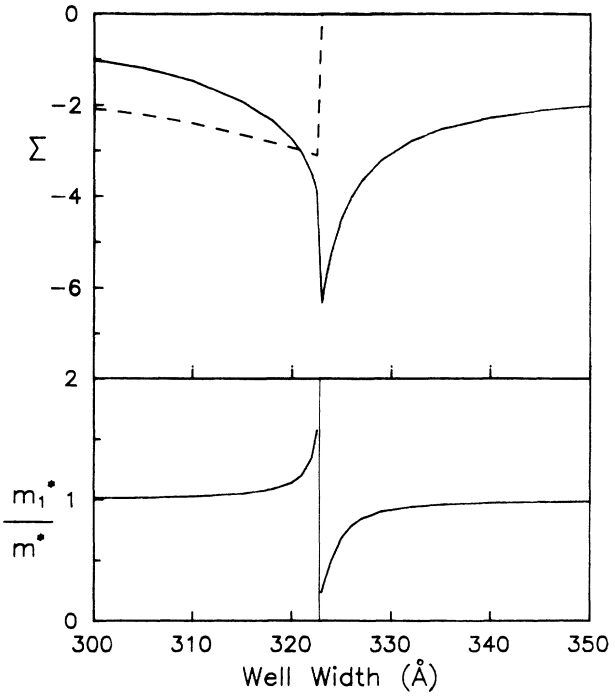

FIG. 3. Upper panel: the real part (solid line) and imaginary part (dashed line) of the self-energy of the third subband are plotted as functions of the well width. Lower panel: the ratio between the effective masses of the third subband with and without electron-phonon coupling is plotted against the well width.

portion with finite $\mathbf{p}_{\parallel}$ was depressed more because it was closer to resonance. As a result, the parabolic band was flattened and the effective mass became greater. The variation of effective mass is quite significant. It will be interesting to see this in the experiments.

From Figs. 2 and 3, we see that the coupling of the third subband is stronger than that of the second subband. The reason is that the former involves symmetric phonons. It has the smallest wave vector $\mathbf{k}_n$ due to confinement and hence gives the strongest Coulomb interaction [see Eq. (22)].

Finally we comment on the screening effect in our calculation. The simplest way of taking screening into account is by replacing the Coulomb potential $1/(q_{\parallel}^2+k_n^2)$ with $1/(q_{\parallel}^2+k_n^2+q_{\mathrm{TF}}^2)$, where q_{TF} is the Thomas-Fermi wave vector. For an electron density around $10^{12}/\mathrm{cm}^2$, q_{TF} is of the same order as k_1 and k_2. Thus screening roughly reduces the electron-phonon coupling by a half. Another important effect of the electron concentration in the quantum well is that when the lower portion of the first subband is occupied, the electrons in the higher subband cannot drop to this portion by emitting a phonon. This will affect very significantly the self-energy near resonance.

In conclusion, we have derived the electron-phonon interaction expression for arbitrary wave forms of electrons and phonons. It can readily be reduced to a form for two-dimensional systems. Then it can be applied to electrons in a quantum well where resonance occurs. The self-energy was calculated. Both energy shift and level broadening are quite significant. Resonance also has a large effect on the effective mass. All of above are not difficult to find in the experiments.

ACKNOWLEDGMENTS

This work is supported in part by the National Science Council of the Republic of China under Contracts No. NSC79-0208-M002-51 and No. NSC79-0208-M002-36.

[1]D. M. Larsen, Phys. Rev. B **30**, 4807 (1984).
[2]S. Das Sarma and B. A. Mason, Ann. Phys. (N.Y.) **163**, 78 (1985).
[3]R. J. Nicholas, L. C. Brunel, S. Huant, K. Karrai, J. C. Portal, M. A. Brummel, M. Razeghi, K. Y. Cheng, and A. Y. Cho, Phys. Rev. Lett. **55**, 883 (1985).
[4]H. Sigg, P. Wyder, and J. A. A. Perenboom, Phys. Rev. B **31**, 5253 (1985).
[5]W. Seidenbusch, E. Gornik, and G. Weimann, Physica B+C (Amsterdam) **134B**, 314 (1985).
[6]U. Merkt, M. Horst, T. Evelbauer, and J. P. Kotthaus, Phys. Rev. B **34**, 7234 (1986).
[7]N. Sawaki, J. Phys. C **19**, 4965 (1986).
[8]M. A. Brummel, R. J. Nicholas, M. A. Hopkins, J. J. Harris, and C. T. Foxon, Phys. Rev. Lett. **58**, 77 (1987).
[9]B. A. Mason and S. Das Sarma, Phys. Rev. B **35**, 3890 (1987).
[10]M. H. Degani and O. Hipólito, Phys. Rev. B **35**, 7717 (1987).
[11]B. K. Ridly, Phys. Rev. B **39**, 5282 (1989).
[12]F. M. Peeters, X.-G. Wu, and J. T. Devreese, Surf. Sci. **196**, 437 (1988).
[13]C. T. Giner and F. Comas, Phys. Rev. B **37**, 4583 (1988).
[14]N. Mori, K. Tanignchi, C. Hamaguchi, S. Sasa, and S. Hiyamizu, J. Phys. C **21**, 1791 (1988).
[15]S.-W. Gu, Y.-C. Li, and L.-F. Zheng, Phys. Rev. B **39**, 1346 (1989).
[16]N. Mori and T. Ando, Phys. Rev. B **40**, 6175 (1989).
[17]D. L. Lin, R. Chen and Thomas F. George, *Symposium on Quantum Wells and Superlattices Physics III* [Proc. Soc. Photo-Opt. Instrum. Eng. (to be published)].
[18]M. P. Chamberlain and M. Babiker, J. Phys. Condens. Matter **1**, 1181 (1989).
[19]M. P. Chamberlain and M. Babiker, Solid State Electron. **32**, 1675 (1989).
[20]M. Born and K. Huang, *Dynamical Theory of Crystal Lattices* (Clarendon, Oxford, 1968).
[21]T. Ando and S. More, Surf. Sci. **113**, 124 (1982).
[22]M. Babiker, J. Phys. C **19**, 683 (1986).
[23]Actually, we have used $\omega_{q_{\parallel},n}$ in the second line of Eq. (21), but have not found any noticeable difference.
[24]B. D. McCombe (private communication).
[25]See, for example, Ref. 2.